

The Electronic Structure of CaCuO₂ From the B3LYP Hybrid Functional

Xiao-Bing Feng^{1,2} and N. M. Harrison^{1,3}

¹Department of Chemistry, Imperial College of Science, Technology and Medicine, London, SW7 2AY, UK

²Department of Physics, Dalian Railway Institute, Dalian, 116028, P. R. China

³CLRC, Daresbury Laboratory, Computational and Material Science Department, Daresbury, Warrington, WA4 4AD, UK

Abstract

The electronic structure of the infinite layer compound CaCuO₂ has been calculated with the B3LYP hybrid density functional. The mixing of the Hartree-Fock exchange in the exchange-correlation energy separated the bands crossing Fermi energy to form an antiferromagnetic insulating ground state of charge transfer type. The complete elimination of the self-interaction through the exact exchange and the optimized gradient-corrected correlation energy significantly improved theoretical results. The theoretical energy gap and magnetic moment are in excellent agreement with the experiments. The ratio of intralayer to interlayer magnetic coupling constants and lattice parameters are also in good accordance with the experiments. Some characteristics of the electronic structure of insulating Sr₂CuO₂Cl₂ from angle-resolved photoemission experiments are observed in the B3LYP band structure for CaCuO₂.

PACS numbers: 71.15.Mb; 71.27.+a; 74.25.Jb

As a parent compound of high temperature superconductors (HTSC), the infinite layer material CaCuO₂ [1] has a simple structure and a high transition temperature when doped to optimum hole density [2, 3]. Similar to La₂CuO₄ and YBa₂Cu₃O₆, CaCuO₂ has an insulating three-dimensional antiferromagnetic (AFM) ground state [4], with energy gap $\Delta = 1.5$ eV [5] and magnetic moment $\mu = 0.51 \mu_B$ [4]. Although the ratio of interlayer to intralayer magnetic coupling is one order of magnitude higher than that in La₂CuO₄ and YBa₂Cu₃O₆, the ratio is still very low. The nuclear magnetic resonance experiment on Cu in Ca_{0.85}Sr_{0.15}CuO₄ shows that the interlayer coupling is about two orders of magnitude less than the intralayer one [6].

The electronic structure of CaCuO₂ has been investigated by several theoretical methods, such as LAPW [7], LMTO-ASA [8], FLMTO [9]. These LSDA-based methods failed to give the correct ground state, as in the case of other HTSCs [10]. Later, it was found that the failure was due to the self-interaction inherent in the LSDA density functional, which tends to delocalize the electrons. The self-interaction correction (SIC) method gave correct AFM insulating ground state with $\mu = 0.58 \mu_B$ and $\Delta = 0.84$ eV [11]. The LSDA+*U* method also generated correct ground state, with $\Delta = 2.1$ eV and $\mu = 0.66 \mu_B$ for $U = 7.5$ eV [12] and $\Delta = 1.96$ eV and $\mu = 0.71 \mu_B$ for $U = 5$ eV [13]. Although the two approaches recovered the correct ground state, their quantitative comparisons with the experiments were not satisfactory.

In this paper we study the electronic structures of CaCuO₂ with the so-called B3LYP hybrid density functional. The hybrid functional was very successful in the thermochemistry of atoms and molecules [14]. Later, the hybrid functional was applied to some periodic systems [15, 16]. The argument for mixing the Hartree-Fock (HF) exchange in the exchange-correlation energy

E_{XC} is based on the adiabatic connection formula [14],

$$E_{XC} = \int_0^1 U_{XC}^\lambda d\lambda, \quad (1)$$

where λ is the electron-electron interaction parameter, with $\lambda = 1$ corresponding to the real interaction and $\lambda = 0$ a system of noninteracting electrons. U_{XC}^λ is the potential energy of the exchange-correlation at any λ . In the case of $\lambda = 0$ U_{XC}^0 is the HF exchange energy of the corresponding noninteracting system. The weights for the gradient-corrected correlation energy, local exchange energy and the exact HF exchange terms were determined by a linear least-square fitting of the thermochemical properties of some atoms and molecules. The atom with highest atomic number used in the fitting is Cl. No atoms with d or higher shells were used. 20% mixing of the exact HF exchange energy in the E_{XC} gives theoretical results in good agreement with experiments. In the B3LYP scheme the Perdew-Wang [17] gradient-corrected correlation energy is replaced by Lee-Yang-Parr correlation energy [18].

The final exchange-correlation energy functional reads

$$E_{XC} = E_X^{LSDA}(1 - a_0) + a_0 E_X^{exact} + a_X \Delta E_X^{B88} + E_C^{LSDA} + a_C \Delta E_C^{LYP}, \quad (2)$$

in which the local spin density functional of Vosko, Wilk and Nusair [19] is used for E_X^{LSDA} and E_C^{LSDA} . E_X^{exact} is the exact nonlocal HF exchange energy. ΔE_X^{B88} and ΔE_C^{LYP} are the Becke's [20] and Lee-Yang-Parr's gradient corrections for the local exchange and correlation energies, respectively. The optimum values for the parameters a_0 , a_X and a_C are 0.20, 0.72, and 0.81, respectively [14].

In this paper the calculations are carried out with CRYSTAL package [21]. The basis vectors for expanding the Kohn-Sham orbitals are Bloch functions composed

of localized contracted basis sets[22]. All-electron basis sets for Ca, Cu and O ions are of the form of 86-511G, 86-411(41d)G and 8-411G, respectively.

In the calculations 75 points in the irreducible part of the first Brillouin zone(FBZ) were used. We adopt the 7, 7, 7, 7 and 14 as the integral tolerances to obtain high precision in monoelectronic and bielectronic integrals. Also a strict criteria for convergence, i.e. when the difference between two consecutive root-mean-squared values of the density matrix elements is less than 10^{-9} the convergence is assumed, is used to make the magnetic moments on Cu sites converge. Different magnetic states, i.e. metallic(without spin polarization), ferromagnetic, two-dimensional(2D) and three-dimensional(3D) antiferromagnetic structures, were checked to find the ground state magnetic configuration. For comparisons, the unrestricted Hartree-Fock(UHF) and general gradient-corrected LSDA(LSDA+GGA) calculations were also carried out with the same basis sets. We also performed structural optimization for the 3D AFM supercell. The optimization is implemented with Domin algorithm and the P4/mmm symmetry is preserved.

Our results show that the 3D AFM state has the lowest energy, i.e. the B3LYP hybrid functional could predict correct ground state magnetic configuration. The energy difference per unit cell between the ferromagnetic and the 2D AFM(antiferromagnetic order in the CuO₂ plane and ferromagnetic order in the Z direction) ground state is 0.285 eV. The 2D and 3D AFM states has nearly the same energies, with the energy of 3D AFM state is only 0.00164 eV lower than that of 2D AFM state. The energies of different magnetic configurations could be described by the Ising model,

$$E = \sum_{\langle ij \rangle} J_{ij} S_i S_j. \quad (3)$$

The intralayer coupling constant J_{\parallel} and interlayer coupling constant J_{\perp} could be obtained from the energy differences of the three different magnetic states. One can easily get $J_{\parallel} = [E_{FM} - E_{2DAFM}]/4$ and $J_{\perp} = [E_{2DAFM} - E_{3DAFM}]/2$, in which E_{FM} , E_{2DAFM} and E_{3DAFM} are the energies of FM, 2D AFM and 3D AFM states, respectively. The theoretical results are $J_{\parallel} = 825.5\text{K}$ and $J_{\perp} = 9.49\text{K}$. The ratio J_{\perp}/J_{\parallel} is 1.1%, which is in good agreement with the experimental result that the interlayer magnetic coupling is about 2 orders of magnitude weaker than the intralayer coupling[6].

The optimized lattice parameters for the supercell are $a=5.563\text{\AA}$ and $c=6.536\text{\AA}$. The results are about 2% larger than the experimental values[1]. The precision is comparable to LDA computations for conventional materials. In addition, Table I shows that the B3LYP theoretical magnetic moments and energy gap obtained with experimental and theoretical lattice parameters are in excellent agreement with the experiments[4, 5]. As mentioned above the optimum parameters were obtained with atoms and molecules without d-electrons, so the excellent agreement between the theory and experiments was unex-

TABLE I: The energy gaps Δ (in eV) and magnetic moments μ (in μ_B) from different theoretical schemes are compared with experiments for CaCuO₂ and La₂CuO₄. The results with superscripts a and b are obtained using experimental and optimized lattice parameters, respectively.

	UHF	SIC-LSD	LSDA+U	B3LYP	Expt
CaCuO ₂ (Δ)	14.9	0.84 ^[11]	2.1 ^[12] 1.96 ^[13]	1.54 ^a 1.50 ^b	1.5 ^[5]
CaCuO ₂ (μ)	0.89	0.58 ^[11]	0.66 ^[12] 0.71 ^[13]	0.51 ^a 0.51 ^b	0.51 ^[4]
La ₂ CuO ₄ (Δ)	17 ^[27]	2.1 ^[28] 1.04 ^[26]	1.65 ^[29]	2.0 ^[16]	2.0 ^[30]

pected because of the strong localized character of d orbitals. But from the study of pseudopotentials one knows that the 2p orbitals in the first-row atoms also pose problems, these orbitals have also localized character because of the lack of orthogonal repulsions. So, if there are enough variational freedoms in the B3LYP hybrid functional to correctly describe atoms with 2p shell then it could be applied to systems with 3d electrons.

The large energy gap of the UHF results from the lack of correlation, i.e. the interaction is not screened. As can be seen in Table I that the UHF gaps for both CaCuO₂ and La₂CuO₄ are about one order of magnitude larger than the experimental results. It is also much larger than the usual cases, which means that the correlation effects are more important in these materials.

The projected densities of states(DOSs) are shown in Fig. 1 and the band structures along the high symmetry lines are shown in Fig. 2(a). These results are obtained with experimental structural parameters. The results show that CaCuO₂ is a charge transfer insulator. This is similar to the case of transition metal monoxides[15]. As shown in Fig. 1 the main components at the top of the valence bands and the bottom of the conduction bands are Cu 3d_{x²-y²} and O 2p_{x(y)}. Though the spectral weight at the bottom of the conduction bands is mostly of Cu 3d_{x²-y²} nature, there is a significant ingredient of O 2p_{x(y)} at the top of the valence bands. Because of the lack of apical oxygens in CaCuO₂ the bonding along the Z direction is weak, which is different from La₂CuO₄, where significant Cu 3d_{z²}/O 2p_z components are existent at the top of the valence bands[16]. The result suggests that the Cu 3d_{z²}/O 2p_z components in La₂CuO₄ may not be essential to the high temperature superconductivity of the system.

One may also notice that some features in Fig. 2(a) are in good agreement with the angle-resolved photoemission(ARPES) experiments on the insulating Sr₂CuO₂Cl₂[31]. Sr₂CuO₂Cl₂ has a structure similar to La₂CuO₄, with the apical oxygens in La₂CuO₄ replaced by Cl[32]. The X and M points in Fig. 2(a) correspond to the ($\pi/2$, $\pi/2$) and (π , 0) points in the FBZ of the CuO₂ plane, respectively. The (π , π) point in the ARPES

experiments is equivalent to Γ point in Fig. 2(a). The ARPES experiments show that the valence band top is at $(\pi/2, \pi/2)$ and there is a nearly isotropic dispersion around this point. The dispersion from $(\pi, 0)$ to $(0, 0)$ is flat and the dispersion from $(\pi, 0)$ to $(0, \pi)$ is similar to the one from $(0, 0)$ to (π, π) . All these characteristics are consistent with our results, as can be seen in Fig. 2(a). Due to the folding-up of the FBZ in the case of the AFM supercell, there are two nearly degenerate bands around X points. Although the dispersion along the Γ -X-M direction in Fig. 2(a) is stronger than experimentally observed, a better agreement with experiments may be expected by applying the method to $\text{Sr}_2\text{CuO}_2\text{Cl}_2$.

To see the effect of the mixing of the exact exchange the LSDA+GGA band structure is shown in Fig. 2(b) for comparison. The same supercell and same functionals for GGA corrections were used in the LSDA+GGA and the B3LYP calculations. From Fig. 2(a) and Fig. 2(b) one can see that the mixing of the exact exchange results in no significant change of the dispersions and relative positions of the bands far from Fermi energy E_F . But the important effect of mixing exact exchange is that two bands, which cross E_F , are separated from the other two bands. The separated two bands have no overlap with the other conduction bands, which is different from the LSDA+ U results[12, 13]. In the LSDA+ U scheme there are also two separated bands composed of Cu $3d_{x^2-y^2}$ and O $2p_{x(y)}$ antibonding states, but the two bands are overlapped with other conduction bands[13].

Except the difference mentioned above between the B3LYP and the LSDA+ U schemes, some essential characters are shared by the two approaches. The reduced energy gap results from upward shift of part of Cu $3d_{x^2-y^2}$ and O $2p_{x(y)}$ spectral weights, and this part of spectral weights have similar width in both schemes. Also the most important projected DOSs for Cu $3d_{x^2-y^2}$ and O $2p_{x(y)}$ have the same characters[12]. Although the LSDA+ U captures the essential physics in strongly correlated systems its quantitative results are not as good as the B3LYP. The reason may be due to the simple mean-field treatment of the Hubbard U term in the LSDA+ U . Recently, Mazin *et al.* have shown that the LSDA+ U failed for moderately-correlated metal, such as FeAl[23].

In the LSDA+ U scheme it is easy to see the reason why the bands crossing E_F were separated to form a gap. The additional orbital dependent potential splits a band into Hubbard subbands, with separation equal to approximately the screened on-site Coulomb repulsion U . The SIC approach restores the localized character of d orbitals, thus introducing strong on-site Coulomb repulsion. In the studies of the Mott insulators it was found that the simple UHF can give qualitatively correct

results, whereas more advanced DFT methods failed[24]. The reason is that in the UHF there is no self-interaction.

In our UHF calculation for CaCuO_2 the energy gap is about one order of magnitude larger than the experimental result. It's expectable that small amount of mixing of the exact exchange would reduce the unphysical large gap to the experimental value while maintaining the correct ground state magnetic configuration. But in the B3LYP approach it is not very clear why only 20% mixing of the exact exchange into the GGA corrected LSDA can greatly change the LSDA+GGA results. To see the point one can rewrite Eq. (2) as

$$E_{XC} = E_X^{exact} + (1 - a_0)(E_X^{LSDA} - E_X^{exact}) + a_X \Delta E_X^{B88} + E_C^{LSDA} + a_C \Delta E_C^{LYP}. \quad (4)$$

Instead of only 20% exact exchange one can view the B3LYP as incorporating 100% exact exchange, and treat the second and the third terms as additional contributions to the correlation energy. So, with the exact exchange, where the self-interaction is completely excluded, and additional variation freedoms for correlation energy one should expect that the method would give better results than the LSDA+GGA and the UHF approaches, in the latter case the correlation energy is totally discarded.

One may view the B3LYP hybrid functional as a much improved energy functional towards the exact one. For a specific class of materials better results can be obtained by reoptimizing the parameters appearing in the correlation energy and by adding additional functionals. It is also interesting to test if the B3LYP functional could be successfully applied to moderately-correlated and doped strongly correlated systems. Muscat *et al.* have applied the B3LYP to materials of different types of bonding[15]. The theoretical energy gaps are in good agreement with experiments, and the band structure for Si is also in good accordance with experiments and other theoretical methods, such as quantum Monte Carlo. For the Mott insulator NiO the B3LYP also generated much better energy gap than the LSDA+ U [25] and the SIC-LSD[25, 26]. So, one can expect more successful applications of the method to other materials.

To conclude, the B3LYP scheme has been applied to CaCuO_2 . The mixing of the exact exchange eliminated the self-interaction and caused the band separation about the Fermi energy compared with the LSDA+GGA method. The magnetic moment and energy gap are in excellent agreement with experiments. Some of the structural and magnetic properties are also in good agreement with experiments. The ARPES characteristics on $\text{Sr}_2\text{CuO}_2\text{Cl}_2$ are observed in our calculations on CaCuO_2 .

[1] T. Siegrist *et al.*, Nature **334**, 231(1988).
[2] J. H. Schon *et al.*, Nature **414**, 434 (2001).
[3] M. Azuma *et al.*, Nature **356**, 775 (1992).

[4] D. Vaknin *et al.*, Phys. Rev. B **39**, 9122 (1989).
[5] Y. Tokura, S. Koshihara, and T. Arima, Phys. Rev. B **41**, 11657 (1990).

- [6] A. Lombardi *et al.*, Phys. Rev. B **54**, 93 (1996).
- [7] L. F. Mattheiss and D. R. Hamman, Phys. Rev. B **40**, 2217 (1989); D. Singh *et al.*, Physica B **163**, 470 (1990).
- [8] M. A. Korotin and V. I. Anisimov, Mater. Lett. **10**, 28 (1990).
- [9] D. L. Novikov, V. A. Gubanov, and A. J. Freeman, Physica C **210**, 301 (1993).
- [10] W. E. Pickett, Rev. Mod. Phys. **61**, 433 (1989).
- [11] D. Singh, W. E. Pickett, and H. Krakauer, Physica C **162-164**, 1431 (1989).
- [12] Vladimir I. Anisimov, Jan Zaanen, and Ole K. Andersen, Phys. Rev. B **44**, 943 (1991).
- [13] Hua Wu *et al.*, J. Phys.: Condens. Matter **11**, 4637 (1999).
- [14] Axel D. Becke, J. Chem. Phys. **98**, 5648 (1993).
- [15] J. Muscat, A. Wander, N. M. Harrison, Chem. Phys. Lett. **342**, 397 (2001).
- [16] J. K. Perry, J. Tahir-Kheli, and W. A. Goddard, Phys. Rev. B **63**, 144510(2001).
- [17] J. P. Perdew, in *Electronic Structure of Solids*, edited by P. Ziesche and H. Eschrig (Academic Press, Verlag, Berlin, 1991).
- [18] Chengteh Lee, Weitao Yang, and Robert G. Parr, Phys. Rev. B **37**, 785 (1988).
- [19] S. H. Vosko, L. Wilk, and M. Nusair, Canadian J. Phys. **58**, 1200 (1980).
- [20] A. D. Becke, Phys. Rev. A **38**, 3098 (1988).
- [21] V. R. Saunders *et al.*, CRYSTAL98 User's Manual (University of Torino, Torino, 1998).
- [22] http://www.chimifm.unito.it/teorica/crystal/Basis_Sets/mendel.html
- [23] I. I. Mazin *et al.*, arXiv:cond-mat/0206548.
- [24] N. M. Harrison *et al.*, in *The Metal-Non Metal Transition in Macroscopic and Microscopic Systems* **356** (1735) p.75 P. P. Edwards *et al.* (Eds), Phil. Trans. A., (1997)
- [25] S. L. Dudarev *et al.*, Phys. Stat. Sol. (a) **166**, 429 (1998).
- [26] A. Svane, Phys. Rev. Lett. **68**, 1900 (1992).
- [27] Y. -S. Su *et al.*, Phys. Rev. B **59**, 10521 (1999).
- [28] W. M. Temmerman, Z. Szotek, and H. Winter, Phys. Rev. B **47**, 11533 (1993).
- [29] M. T. Czyzyk and G. A. Sawatsky, Phys. Rev. B **49**, 14211 (1994).
- [30] J. M. Ginder *et al.*, Phys. Rev. B **37**, 7506 (1988).
- [31] B. O. Wells *et al.*, Phys. Rev. Lett. **74**, 964(1995); C. Kim *et al.*, *ibid.* **80**, 4245(1998).
- [32] L. L. Miller *et al.*, Phys. Rev. B **41**, 1921(1990).

Figure Captions

Fig. 1 The projected densities of states of Cu 3d, O 2p and Ca 3sp partial waves in a $\sqrt{2} \times \sqrt{2} \times 2$ supercell of CaCuO₂. All the DOSs are for spin-up electrons and the magnetic moment of Cu is $-0.51\mu_B$.

Fig. 2 (a). The B3LYP energy bands of a $\sqrt{2} \times \sqrt{2} \times 2$ supercell of CaCuO₂. (b). The LSDA+GGA band structure of the same supercell. The coordinates of the high symmetry points are $\Gamma = (0, 0, 0)/2$, $M = (1, 1, 0)/2$, $Z = (0, 0, 1)/2$, $R = (0, 1, 1)/2$ and $A = (1, 1, 1)/2$. The bands are for spin-up electrons.

Figure 1

Xiao-Bing Feng et al.

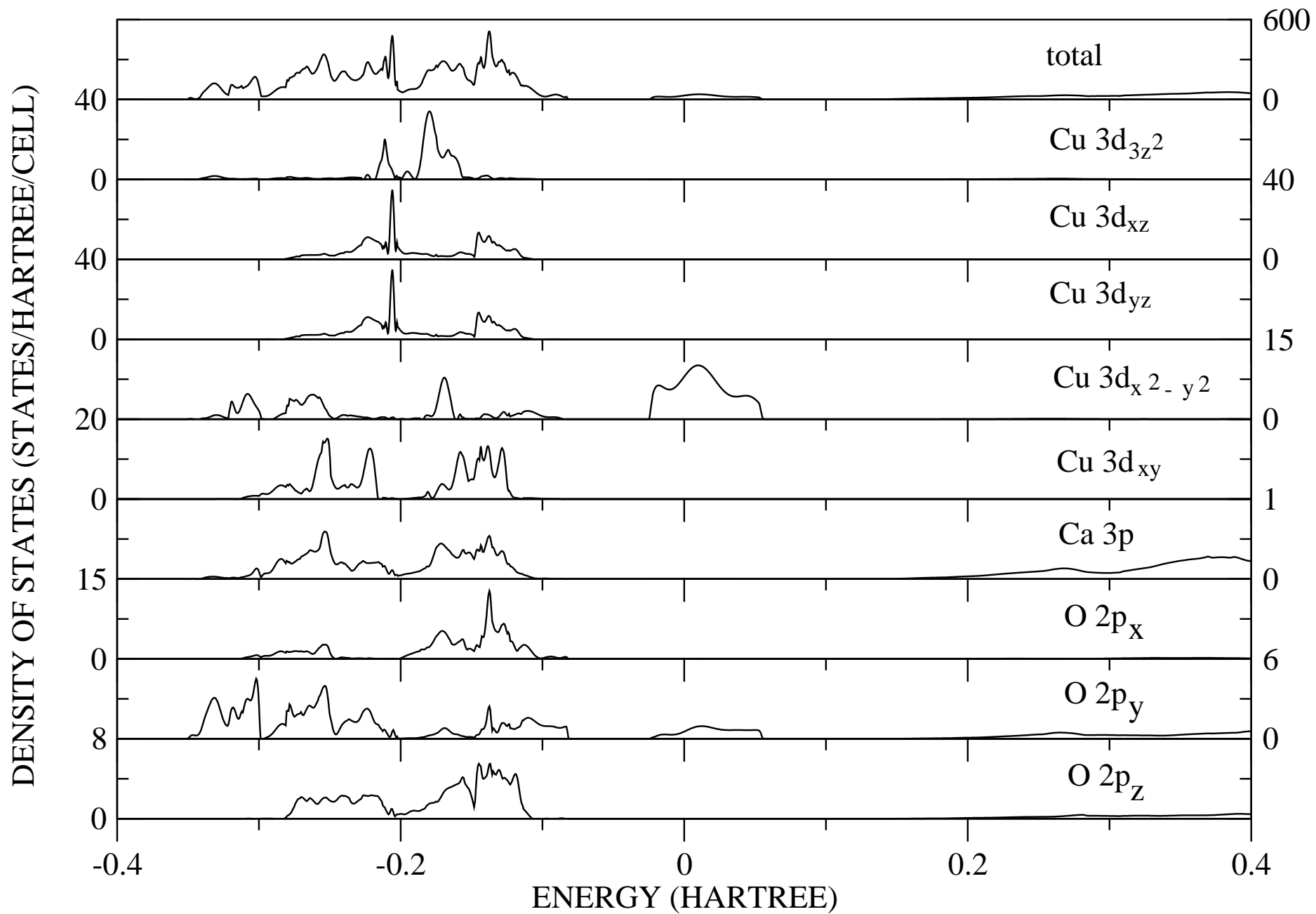


Figure 2(a)

Xiao-Bing Feng et al.

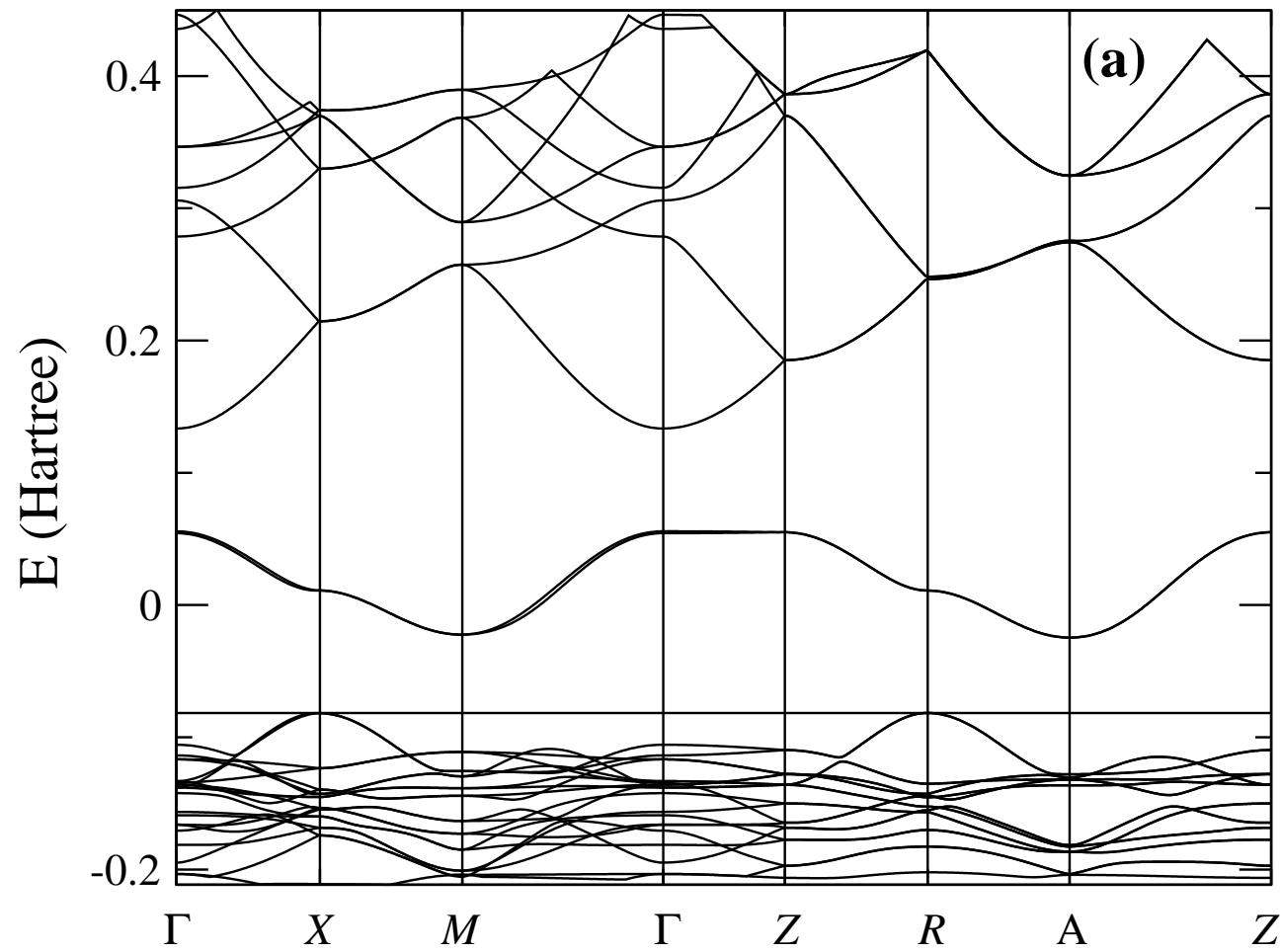


Figure 2(b)

Xiao-Bing Feng et al.

